Translational Relevance

For the prediction of the therapeutic efficacy of molecularly targeted medicines, it is ideal to evaluate the therapeutic mechanisms in individual patients. Therefore, it is highly significant to evaluate the drug functions in fresh tumor cells near *in vivo* conditions. To date, invasiveness and a great deal of time and effort have been unavoidable in such evaluations. In this study, we developed a rapid evaluation system for complement-dependent cytotoxicity of rituximab by using living cell–imaging technology. The advantages of imaging-based procedures include the need for only a minimal amount of specimen as well as its rapidity. Our system enabled reproducible evaluation even from tiny specimens and distinguished between responsive and refractory groups of rituximab-containing chemotherapy. This evaluation system may be easy to apply to antibody medicines other than rituximab and to other mechanism of actions such as antibody-dependent cellular cytotoxicity. Thus, this study may offer the opportunity to evaluate the effect of various antibody drugs in clinical applications.

the mechanisms, apart from ADCC. Several reports have suggested the role of CDC in the clinical efficacy of rituximab (11-13); however, it is a less convincing argument than that for ADCC. To elucidate this question, it is absolutely critical to evaluate the intrinsic CDC susceptibility of freshly obtained lymphoma cells from patients. To do so, a rapid, reproducible, and sufficiently smaller-scaled assay system is essential. To address this, we established a novel procedure to quantify the susceptibility of patient-derived lymphoma cells to CDC induced by rituximab. We developed a remarkably smaller-scaled assay procedure by using a real-time imaging technique, making it possible to perform multiple measurements with a small portion of the cells derived from lymph node biopsy obtained for diagnosis. In this study, we evaluated the CDC susceptibility of 234 patients with suspected lymphoma, using this new analytic method. Among these cases, as for diffuse large B-cell lymphoma (DLBCL) and follicular lymphoma (FL) in which rituximab-containing chemotherapy is frequently chosen, we further evaluated how much CDC is involved in the therapeutic response.

Materials and Methods

Lymphoma cells from patients. Primary malignant lymphocytes were prepared from lymph node biopsy specimens obtained from patients who had given written informed consent. Briefly, an excised lymph node was minced with scissors, and a mononuclear cell fraction was obtained by centrifugation (1,000 × *g* at 25°C for 30 min) through Ficoll histopaque (Sigma). B-lymphoid tumor cells were further purified by immunomagnetic cell sorting (according to the manufacturer's instructions) using an anti-human CD19 antibody conjugated to magnetic beads (MACS System, Miltenyi Biotec) from a small part of the mononuclear cells. The study was approved by the Institutional Review Board of the Japanese Foundation for Cancer Research.

Antibodies. Rituximab was purchased from Chugai Pharmaceutical Co., Ltd., and dialyzed thrice into PBS. For a control study, the $F(ab')_2$ fragment of rituximab was prepared by treating the antibody with immobilized pepsin and separating the resulting $F(ab')_2$ fragments on an immobilized protein A column (Pierce Biotechnology, Inc.). Purified rituximab and its $F(ab')_2$ fragment were labeled with Alexa 488 (Molecular Probes) according to the manufacturer's instructions. FITC-labeled anti-human CD19 mouse monoclonal antibody and PE-labeled anti-CD20 mouse monoclonal antibody were purchased from Becton Dickinson for flow cytometry analysis. Anti-human CD19 Microbeads were purchased from Miltenyi Biotec for immunomagnetic cell sorting.

Live cell imagingased CDC assay. Forty thousand purified B-lymphoid tumor cells were suspended in 4 μL of RPMI 1640 supplemented with 10% fetal bovine serum, 10 μg/mL of Alexa 488–labeled rituximab, and 5 μg/mL of propidium iodide (PI). The cell suspension was pipetted into a well made of silicon, 2.5 mm in diameter and 2 mm in depth, on a piece of cover glass. Subsequently, the cell suspension was set on the stage of a confocal microscope system (FV-1000; Olympus, Tokyo, Japan) set up in a microscope incubator (Tokken, Chiba, Japan). After 10 min of incubation, 1.0 μL of type AB human serum obtained from a healthy volunteer was added to the well. Cellular alteration immediately after the addition of serum was recorded every 4 s by a time-lapse function at a resolution of 640 × 640 pixels. Using an excitation laser beam with a wavelength of 488 nm, cellular morphology by Nomarski interference contrast imaging, the binding of rituximab at a wavelength of 505 to 525 nm and the PI incorporation into the nuclei of dead cells at a wavelength of 610 to 640 nm were observed. The schema of the principle of this assay is illustrated in Fig. 1. CDC susceptibility index was calculated according to the following formula:

$$\text{CDC susceptibility index (\%)} = \frac{(\text{no. of dead cells at 10 min} - \text{no. of dead cells at 0 min})}{(\text{no. of total cells at 10 min} - \text{no. of dead cells at 0 min})} \times 100$$

Selection of cutoff scores for the CDC susceptibility index. Relevant cutoff scores for predicting therapeutic effect for the CDC susceptibility index were obtained by carrying out receiver-operating characteristic (ROC) curve analysis. In brief, plots of sensitivity and 1– specificity for therapy response were obtained for this index; the closest-to-(0,1) criterion identifies the threshold value.

Statistical procedures. Patients who responded to rituximab-containing chemotherapy were compared with those who were resistant to it. The association of therapy response with the CDC susceptibility index was analyzed using the two-sided Fisher's exact test. $P < 0.05$ was considered significant. A multiple logistic regression analysis was conducted to identify independent predictors of the clinical response to rituximab-containing chemotherapy. A step-down procedure based on a likelihood ratio test was applied, arranged in descending order of importance, with $P = 0.05$ for entry into the model and $P = 0.10$ for removal. Statistical analysis was done using the SPSS software package.

Results

Setting the conditions of the CDC assay. To set the conditions of the assay, CDC susceptibility analysis was done using B-cell NHL cell lines, Daudi, Raji, and Ramos, and by changing several variables. First, to determine the optimal concentration of rituximab, we assessed CDC with various concentrations of rituximab. As a source of complement, human serum at a final concentration of 20% was added to these cell lines suspended in culture medium containing rituximab at a range of 0 to 100 μg/mL. Then, cell death induced during the next 10 min was quantified. CDC reached a plateau at a concentration of >10 μg/mL of rituximab in either cell line (Fig. 2A). To optimize final serum concentration, we next did an assay using various concentrations of human serum with 10 μg/mL of

rituximab. Cell death induced by CDC increased serum concentration dependently, but CDC activity did not reach the plateau at the 0% to 20% level we examined (Fig. 2B). As it was difficult to add more than 20% serum because of the limitations of manipulation, we set the final serum concentration to 20% for subsequent analyses. As to reaction time, cell death in all lines reached a plateau within 10 min after the addition of 20% final concentration of human serum (Fig. 2C). Taking these results into account, we concluded that CDC susceptibility was calculated by measuring the cellular ratio killed in 10 min after the addition of human serum at a final concentration of 20% to the cells suspended in culture medium containing 10 μg/mL of rituximab. To confirm the capability of the assay with clinical specimens, eight cases of freshly obtained lymphoma cells were used to analyze the abovementioned condition. As shown in Fig. 2D, in all eight cases, the proportion of dead cells asymptotically approached a fixed value that varied according to the cases within 10 min. Additionally, under the presence of 10 μg/mL of Alexa 488–labeled human IgG used as a control, a significant increment of cell death was observed in neither case.

The assay system was designed to use a CD19-positive fraction as target cells to reduce the influence of effector cells in the biopsy specimens. To confirm the influence of the effector cells that might not be removed completely in the actual assay, the analysis was carried out using a *F*(ab')2 fragment of rituximab or heat-inactivated serum. The results obtained from lymphoma cells derived from five patients with non-Hodgkin's lymphoma (two cases of DLBCL and three cases of FL) indicated that cell death was extremely decreased by replacing rituximab with its *F*(ab')2 fragment or by heat-inactivation of serum. In both cases, a very small percentage of cells underwent necrotic or apoptotic cell death, but the increase of cell death was not statistically significant and was not more than that observed when human IgG was used as a substitute for rituximab (Supplemental Table S1). These results suggested that the cytotoxicity levels induced by effector cells were almost negligible in our assay system.

Patient characteristics. We evaluated the CDC susceptibility of cells derived from lymph node biopsies taken from 234 cases of suspected lymphoma. The diagnosis breakdown was DLBCL, 23.5%; FL, 20.9%; DLBCL with FL, 2.1%; mantle cell lymphoma, 3.4%; mucosa-associated lymphoid tissue, 4.7%; Burkitt's lymphoma, 0.9%; chronic lymphocytic leukemia/small lymphocytic lymphoma, 2.6%; and cases other than B-cell non-Hodgkin's lymphoma, 42.7%. The cases other than B-cell non-Hodgkin's lymphoma included T-cell lymphomas, nonneoplastic lymph proliferative diseases, lymphadenitis, and Hodgkin's disease. The samples evaluated included 51 patients with DLBCL and 45 patients with FL; patient characteristics are shown in Table 1. Cases were excluded in which

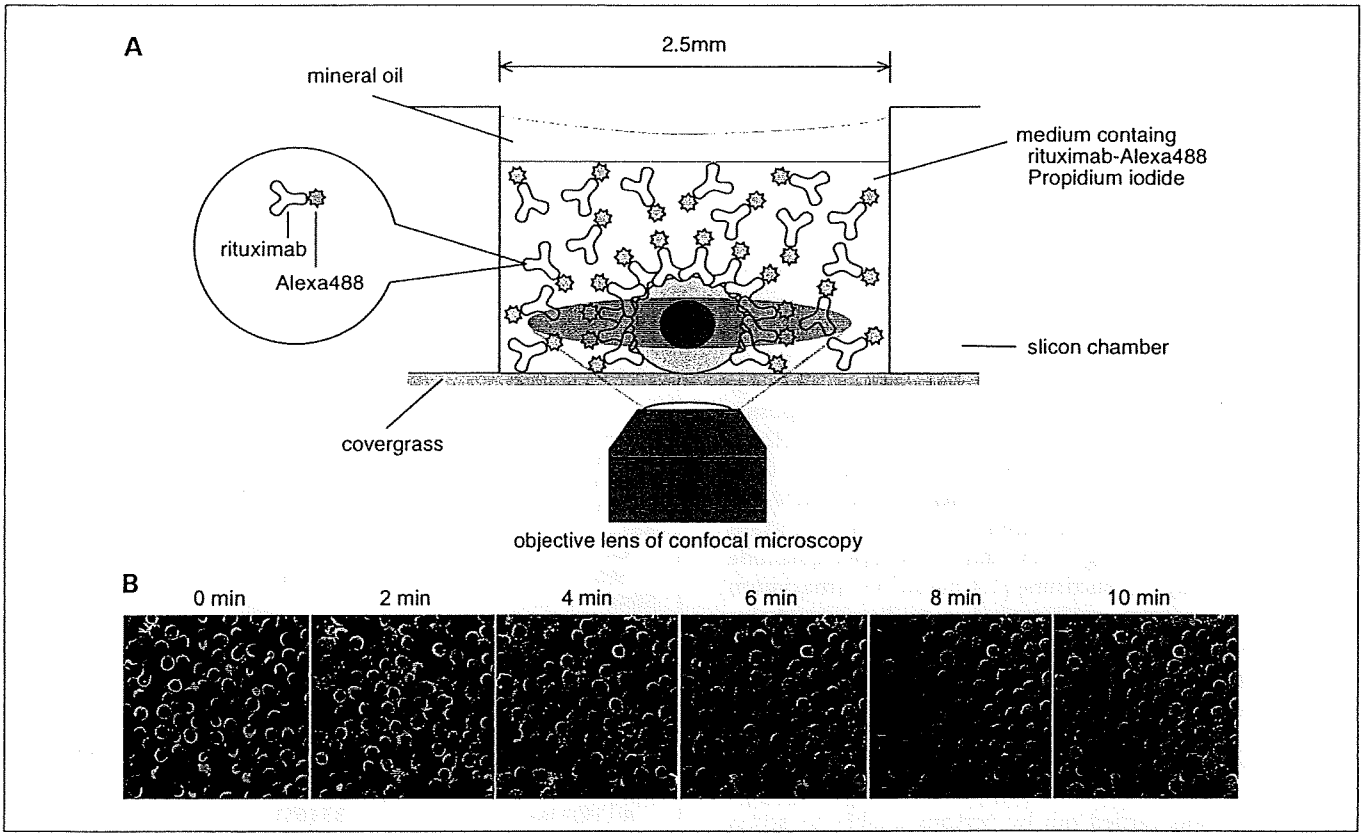

Fig. 1. The principle of imaging-based CDC susceptibility assay. *A*, a schema of CDC susceptibility assay based on living cell imaging. Lymphoma cells were suspended in 4 μL of culture medium containing Alexa 488–labeled rituximab and propidium iodide. The alteration of cellular viability from immediately after the addition of 1 μL of human serum was observed. The CDC-mediated cell killing was distinguished by the incorporation of PI into the nuclei. The background noise from the fluorescent antibody that existed in the culture medium could be excluded by detecting only fluorescent signals around a cellular equatorial plane by using confocal technology. *B*, an example of the assay results from a patient with FL lymphoma. Typical analysis results were shown extracting to images of every 120 s. Green signals, Alexa 488–labeled rituximab; red signals, incorporation of PI into nuclei; bar, 10 μm.

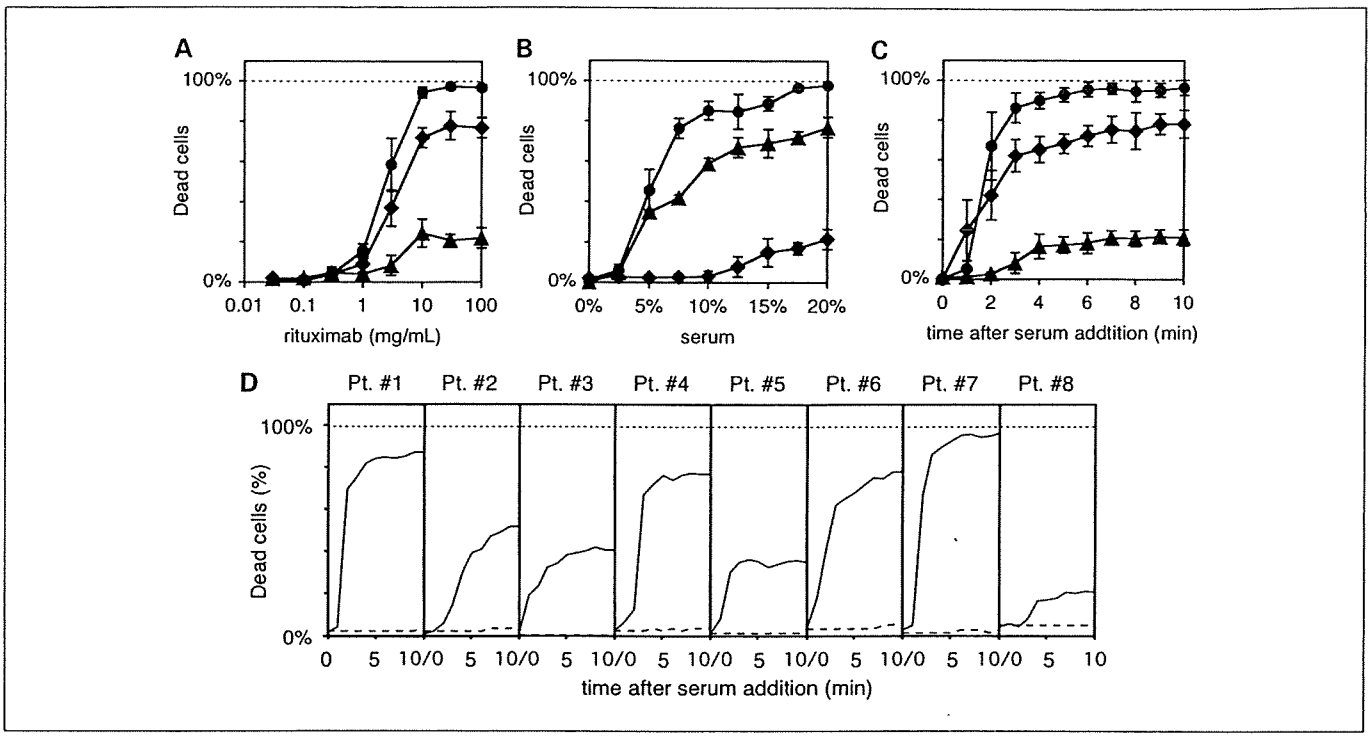

Fig. 2. Rituximab-mediated CDC assays on Burkitt's lymphoma cell lines and primary lymphoma cells. *A*, relationship between the rituximab concentrations and CDC-mediated cell killing in the presence of a final concentration of 20% human serum. Proportions of dead cells were counted and plotted against the rituximab concentrations. Circles, Ramos; diamonds, Raji, triangles, Daudi in *A*, *B* and *C*. *B*, relationship between the serum concentration and CDC-mediated cell killing in the presence of 10 μg/mL of rituximab. Proportions of dead cells were counted and plotted against the serum concentrations. *C*, time course of CDC-mediated cell killing in the presence of 10 μg/mL of rituximab and a final concentration of 20% human serum. Proportions of dead cells were counted and plotted against the time after serum addition. *D*, time course of CDC-mediated cell killing in lymphoma cells derived from biopsy of eight patients. Assay was done in the presence of 10 μg/mL of rituximab and at a final concentration of 20% human serum. All experiments were done in triplicate. Points, mean; bars, SD.

treatment was discontinued for reasons other than disease progression, for example, changing hospitals or developing severe (greater than grade 3/4) adverse events (four cases of DLBCL and four cases of FL).

Rituximabontaining chemotherapies. Thirty-three patients diagnosed with DLBCL and 30 patients with FL received cyclophosphamide, doxorubicin, vincristine, and prednisone (CHOP)–like chemotherapy plus rituximab; 7 patients with DLBCL and 7 with FL received a salvage chemotherapy plus rituximab. The salvage chemotherapy included ifosfamide, carboplatin, and etoposide (ICE) and dexamethasone, cytarabine, and cisplatin (DHAP). Both therapies included rituximab administration at a dose of 375 mg/m^2 i.v. at 1-week intervals of eight cycles. CHOP-like chemotherapy included all regimens with at least standard doses of doxorubicin (50 mg/m^2 i.v., day 1), cyclophosphamide (750 mg/m^2 i.v., day 1), vincristine [1.4 mg/m^2 i.v. (maximum 2 mg), day 1], and prednisone (60 mg/m^2 orally, days 1-5) administered in 3-week cycles.

Measurement of CDC susceptibility of patientrigin lymphoma cells. CD19-positive cells were purified as described in Materials and Methods. The purified cells were mixed with rituximab and human serum on the stage of a confocal microscope, and the CDC susceptibility index was calculated. The CDC susceptibility analysis was carried out by persons unable to access information about diagnosis results or treatment response. Characteristics of CDC susceptibility according to subtype of lymphoma are shown in Fig. 3A. In DLBCL and FL, the CDC susceptibility index had a remarkably wide distribution, from nearly 0% to 100%; means were 54% and 64%, respectively. A comparison with the cases other than B-cell non-Hodgkin's lymphoma showed no significant difference in mean CDC susceptibility; however, it should be noted that relatively low susceptibility cases were included in DLBCL

Table 1. Patient characteristics

Characteristics	DLBCL, *n* = 51	FL, *n* = 45
	n (%)	*n* (%)
Gender		
Female	21 (41)	25 (56)
Male	30 (59)	20 (44)
Age (y)		
<60	14 (27)	23 (51)
≥60	37 (73)	22 (49)
State of disease		
Primary	37 (73)	36 (80)
Relapse	14 (27)	9 (20)
IPI		
Low	31 (61)	20 (44)
Low-intermediate	4 (8)	11 (24)
High-intermediate	8 (16)	11 (24)
High	8 (16)	3 (7)
Treatment		
R-CHOP like	33 (65)	30 (67)
R-ICE	5 (10)	7 (16)
R-DHAP	2 (4)	0 (0)
Without R*	11 (20)	8 (18)

*Chemotherapy regimen without rituximab

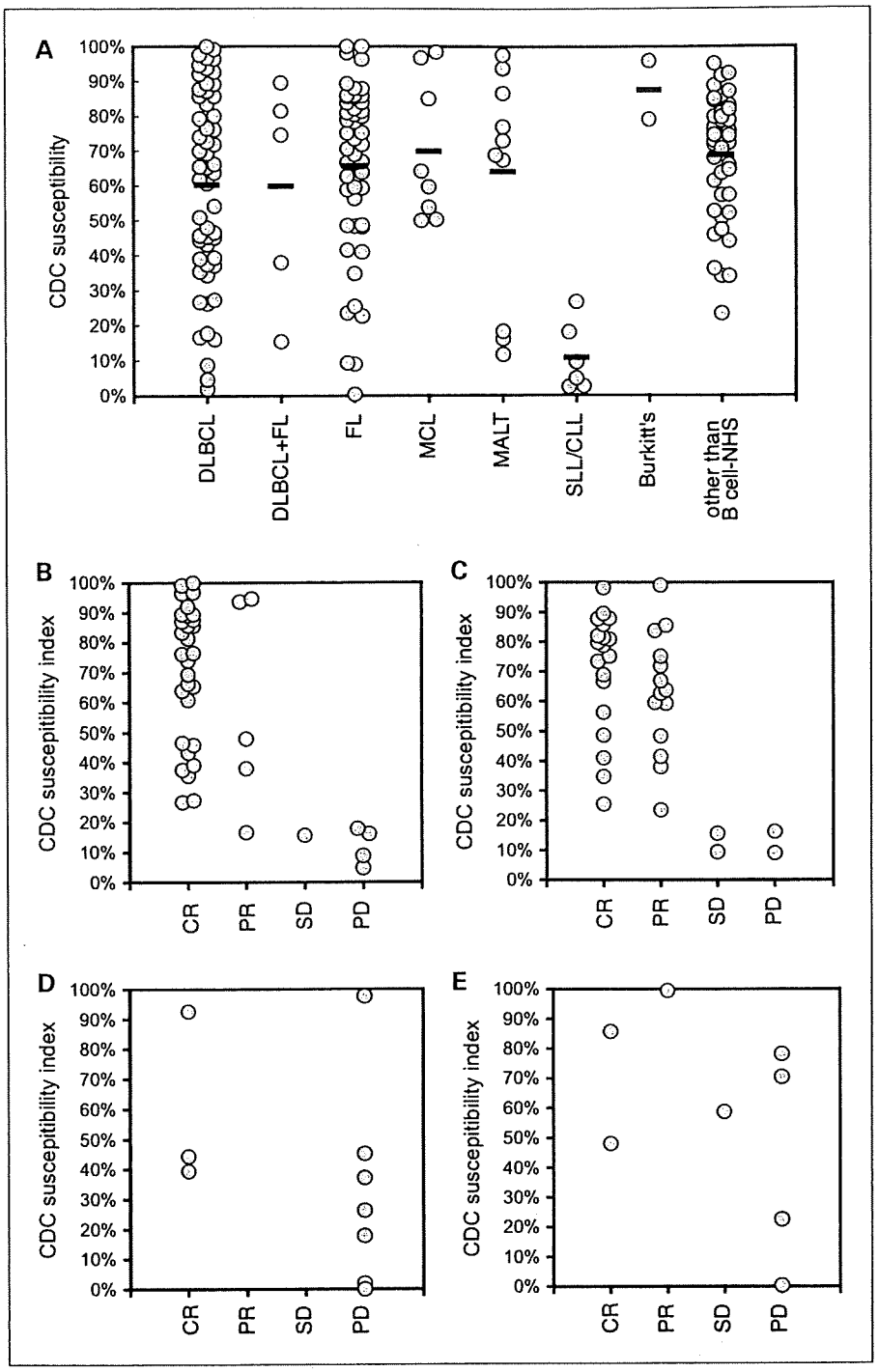

Fig. 3. Profiles of CDC susceptibility index. *A*, a total of 234 cases analyzed for CDC susceptibility were classified in eight categories of disease subtypes. The CDC susceptibility index of each case was plotted. Bar, mean. *B* to *E*, relationship between CDC susceptibility index of lymphoma cells obtained from patients with DLBCL (*B* and *D*) and FL (*C* and *E*) and clinical response of rituximab-containing chemotherapy. Lymphoma cells derived from 40 patients with DLBCL (*B*) and 37 patients with FL (*C*) who received the R+chemotherapy regimen were examined for CDC susceptibility and plotted against prognosis. Similarly, we examined lymphoma cells derived from 10 patients with DLBCL (*D*) and 8 patients with FL (*F*) who received chemotherapy without rituximab.

and FL cases. In mucosa-associated lymphoid tissue and Burkitt's lymphoma, the CDC susceptibility index of all cases we evaluated was >50%, and the means were 69% and 87%, respectively. In contrast, in chronic lymphocytic leukemia/small lymphocytic lymphoma, all cases were <29% with a mean index of 12%. In comparison with a non-B-cell lymphoma case, statistical significant difference was found only in chronic lymphocytic leukemia/small lymphocytic lymphoma cases ($P < 0.001$).

Relationships between CDC susceptibility and response to rituximabontaining chemotherapy. To clarify the association between CDC susceptibility and response to rituximab-containing combination chemotherapy, we did a correlation analysis for DLBCL and FL patients who had undergone CDC susceptibility analysis between January 2005 and December 2007. As for the DLBCL cases that received rituximab combination chemotherapy, 35 patients (87.5%) with complete response (CR) or partial response (PR) were judged effective, whereas 5 patients (12.5%) with stable disease (SD) or progressive disease (PD) were judged not effective. Similarly, for FL cases, 33 patients (89.2%) with CR or PR were judged effective, whereas 4 patients (10.8%) with SD or PD were judged not effective.

To assess the independent contribution of CDC susceptibility to the prediction of clinical response, multiple logistic

regression analysis was done. In the model, we used chemotherapeutic category (induction/salvage) and the International Prognostic Index (IPI) grade as confounding variables. The preceding univariate analysis showed that all these variables were significantly associated with the clinical response ($P < 0.001$, $P = 0.0338$, and $P = 0.0346$ for CDC, IPI, and chemotherapeutic category, respectively). Multiple stepwise logistic regression analysis showed that CDC susceptibility was an independent predictor of clinical response ($P < 0.001$), chemotherapeutic category was also another independent predictor ($P = 0.0473$); on the other hand, the IPI index was not considered to be an independent predictor in this multivariate model.

As CDC susceptibility was reported to be influenced by the target antigen expression levels (14), we then analyzed the relation between rituximab-induced CDC and cell surface CD20 expression levels, and compared their predictive ability. Analysis using Pearson's correlation coefficient indicated a statistically significant correlation between the CDC susceptibility index and CD20 expression level in lymphoma cells derived from patients with both FL and DLBCL (Supplemental Fig. S1; $r = 0.519$, $P < 0.01$, and $r = 0.592$, $P < 0.01$, respectively). ROC curves for both the CDC susceptibility index and CD20 expression levels to distinguish effective (CR + PR) versus noneffective (SD + PD) were produced. The area under the ROC curve for the CDC susceptibility index was significantly larger than that for the CD20 expression level (0.998; 95% confidence interval, 0.992-1.000; and 0.777; 95% confidence interval, 0.578-0.976, respectively; $P = 0.005$), indicating that the CDC susceptibility index was a more powerful discriminator of patients' response than CD20 antigen expression (Fig. 4, *top*).

The ROC curve analysis was further used to calculate the optimal cutoff value of CDC susceptibility for discriminating clinical response. A CDC susceptibility value of 18%, which provided the highest sensitivity and specificity, was selected to categorize lymphoma as high or low CDC susceptibility (Fig. 4, *bottom*). Using this cutoff value, we estimated the prognostic reliability of the CDC susceptibility index in rituximab combination chemotherapy. For DLBCL treated with R-CHOP-like therapy, the response rates were significantly higher in the cases with high CDC susceptibility (96.8% effective) than in those with lower susceptibility (0%; $P < 0.001$; two-sided Fisher's exact test). In addition, in the all-rituximab combination chemotherapy including R-salvage chemotherapy, the cases with high CDC susceptibility exhibited significantly higher response rates (97.2%) than those with a lower CDC index (0%; $P < 0.001$, two-sided Fisher's exact test). Similarly, even in FL, the CDC index showed statistically significant associations with therapy response to both R-CHOP-like therapy and all rituximab combination chemotherapies ($P = 0.0023$ and $P < 0.001$, respectively).

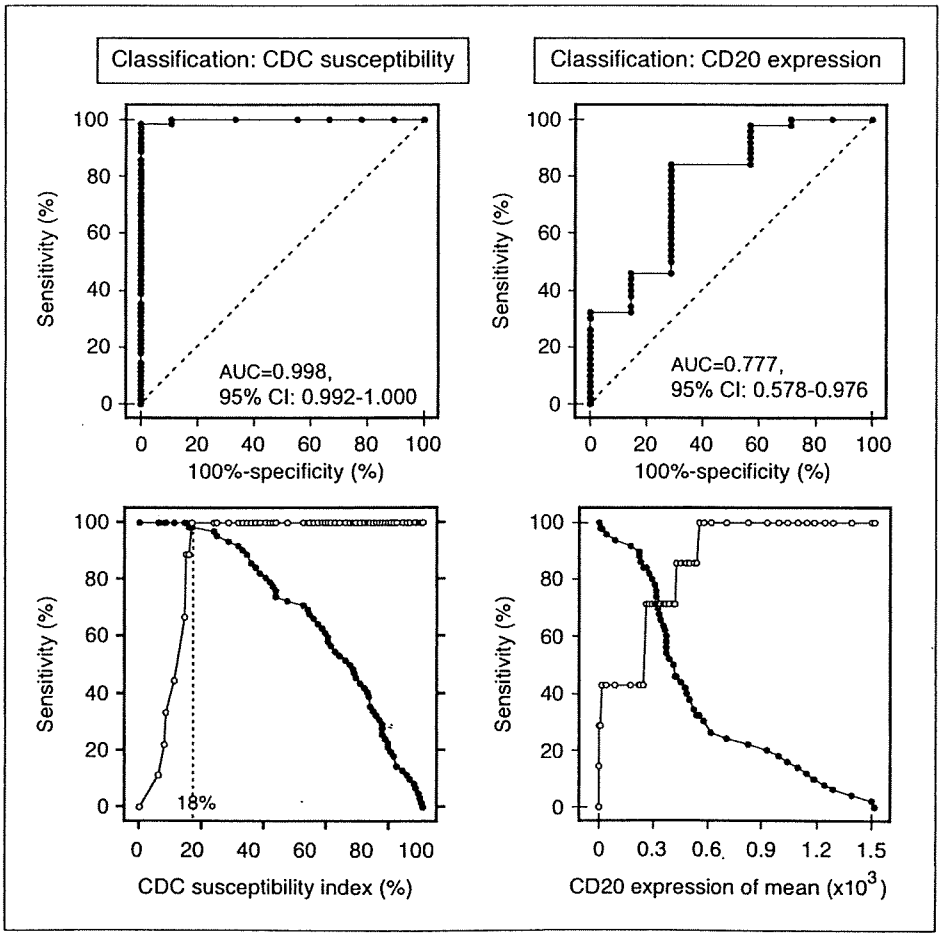

Fig. 4. Comparative analyses between CDC susceptibility and CD20 expression level. ROC curve analysis was done for comparison of predictive power of CDC susceptibility and antigen expression and for optimized threshold value determination. The analyses were conducted on all patients with DLBCL and FL who received the R+chemotherapy regimen, and ROC curves classified by CDC susceptibility index and CD20 expression level were generated (*top*). The areas under the ROC curve (AUC) summarizing the inherent capacity of parameters to discriminate a responder from a nonresponder were calculated. The optimal cutoff value that provides a trade-off between sensitivity (true positives; *solid circles*) and specificity (true negatives; *open circles*) was determined to be 18% for CDC susceptibility from the plot of sensitivity and specificity versus criterion value (*bottom*).

Discussion

Previous studies have suggested that several mechanisms might be involved in the therapeutic efficacy of rituximab, including ADCC (8-10), CDC (4, 11), and the induction of growth arrest or apoptosis (6, 15, 16). Both clinical (17, 18) and experimental (19) studies have offered evidence that ADCC plays an important role. On the other hand, the role of complements in rituximab treatment has been suggested by several preclinical studies. A study using cynomolgus monkeys showed that the ability to deplete CD20-positive cells was almost completely lost when IgG_4, which lacks complement-binding ability, was used in place of IgG_1 (20). In addition, the eradication of syngeneic murine EL4 tumor cells expressing human CD20 by rituximab is dependent on C1q, the first component of the classic pathway, and is independent of natural killer cells (21). Similarly, complement depletion using cobra venom factor markedly reduced the efficacy of rituximab in several lymphoma xenograft models (4). As for clinical evidence, the contribution of CDC to rituximab treatment was indirectly supported by several clinical observations. To give some instances, complement is consumed during rituximab treatment; in some cases, only CD59-positive cells having complement resistance remained after long-term rituximab treatment (11, 22). Thus, several animal models and clinical phenomena suggest the role of complement in rituximab treatment, but no strong, direct evidence of the clinical significance of CDC has yet been shown. It should also be noted that some findings are controversial. Weng and Levy have investigated *in vitro* CDC susceptibility, the expression of CD20, and complement inhibitors CD46, CD55, and CD59 on cryopreserved biopsy specimens from patients with FL, concluding that neither of these variables correlates with the reactivity of rituximab treatment (23).

In the present study, we established a rapid assay method for CDC analysis. Our assay system made it possible to perform an assay with only 40,000 lymphoma cells. In addition, it eliminated the lag-time between incubation and analysis that was unavoidable in other analyses such as flow cytometry methods. These features have contributed highly reproducible multiple measurements, even when only a tiny biopsy specimen could be obtained. Using this system, we evaluated the CDC susceptibility of cells derived from lymphoma patients within 6 hours after the biopsy and analyzed the relationship to clinical response. We succeeded in eliminating most of the influence of effector cells by removing CD19-negative cells from the assay specimen, suggesting that net CDC susceptibility could be estimated. Analysis results on FL and DLBCL suggested a strong correlation between CDC susceptibility and the clinical response to rituximab-containing chemotherapy. This result is inconsistent with the report of Weng and Levy. We believe that the inconsistency was, in part, caused by the method of evaluating CDC susceptibility. Our evaluation method assesses the intrinsic characteristics of the tumor cells by analyzing without cryopreservation after

Table 2. Clinical characteristics in relation to CDC susceptibility in patients with DLBCL and FL

Treatment	CDC susceptibility	Responder	Nonresponder	*P**
DLBCL				
R-CHOP like				
	CDC > 18%	30	0	$P = 0.00067$
	CDC < 18%	1	3	
R+salvage				
	CDC > 18%	5	0	$P = 0.048$
	CDC < 18%	0	2	
R+chemotherapy†				
	CDC > 18%	35	0	$P = 8.0 \times 10^{-6}$
	CDC < 18%	1	5	
Without R‡				
	CDC > 18%	3	4	$P = 0.48$
	CDC < 18%	0	3	
FL				
R-CHOP like				
	CDC > 18%	28	0	$P = 0.0023$
	CDC < 18%	0	2	
R+salvage				
	CDC > 18%	5	0	$P = 0.047$
	CDC < 18%	0	2	
R+chemotherapy†				
	CDC > 18%	33	0	$P = 1.5 \times 10^{-5}$
	CDC < 18%	0	4	
Without R‡				
	CDC > 18%	3	4	$P = 1$
	CDC < 18%	0	1	

*P values were obtained from two-tailed Fisher's exact tests.
†Chemotherapy plus rituximab including R-CHOP–like and R+salvage chemotherapy.
‡Chemotherapy regimen without rituximab.

biopsy and by optimizing assay conditions. Indeed, for some lymphoma cells derived from patients, different results in the CDC susceptibility were observed when the measurement was taken after freeze-thawing versus just after collection (data not shown).

The heterogeneity of the patient backgrounds and of the type of treatment made the data difficult to interpret. Therefore, we did a multivariate analysis to access the independence of CDC susceptibility from the patient background, including the IPI grade and the type of treatment, and found that CDC was a probable independent predictor for effectiveness. In our analysis, the IPI has a significant correlation with clinical response in univariate logistic analysis. However, in multivariate analysis, the IPI did not remain as an independent predictor, perhaps because the data included the salvage therapy. These results suggested that the CDC susceptibility index might be useful in predicting clinical response in both the induction and salvage chemotherapy containing rituximab. In addition, even by being limited to patients who received R-CHOP–like treatment as a first-line chemotherapy, significant correlation was found between CDC and clinical response in both FL and DLBCL (Table 2).

Although a significant correlation between CDC susceptibility index and the cell surface CD20 expression was also found in our analysis, the area under the ROC curve analysis revealed that the CDC susceptibility index was a more powerful discriminator of patients' response than CD20 antigen expression. In the responsive group, the CD20 expression had a wide distribution, including considerably low values (data not shown). These results indicate that cases that will get good therapeutic response in spite of low CD20 expression can be distinguished by CDC susceptibility.

To date, relationships between each mechanism of action, such as ADCC and CDC, have not been clarified completely in the clinical efficacy of therapeutic antibodies. A more detailed mechanism of action in rituximab-containing chemotherapy should be analyzed by evaluating the mutual action of CDC and ADCC. To further understand the relative clinical contribution of both effector mechanisms, we are currently developing an imaging-based reproducible ADCC evaluation system, and we plan to investigate the mutual relationship of ADCC and CDC, as well as the relationship between CDC/ADCC and long-term prognosis such as overall survival or relapse-free survival. These investigations will give us critical information about the exact therapeutic functions of these mechanisms.

The CDC susceptibility distinguished between responsive and refractory groups of rituximab-containing chemotherapy; however, it does not seem to be useful in more detailed classifications, such as complete response or partial response. In addition, the relation to clinical prognosis such as the duration of disease-free survival or overall survival is currently uncertain. In spite of these limitations, our analysis system provides a novel approach to predicting which patients will receive little benefit even if rituximab combination chemotherapy is done. Recently, antibody drugs using different mechanisms for B-cell non-Hodgkin's lymphoma have become increasingly available. Accordingly, it is expected that the prediction of the effects of therapeutic antibodies before the start of therapy will become more and more important in the post-rituximab era, leading to early implementation of optimal therapies, improving clinical outcomes.

In conclusion, we have shown that live cell–imaging is quite useful in improving CDC evaluation methods. The advantages of imaging-based procedures include needing only a minimal amount of specimen as well as rapidity and traceability. All of these features are advantageous to the analysis of clinical specimens. Thus, live cell–imaging may lead to greatly improved clinical evaluations.

Disclosure of Potential Conflicts of Interest

K. Hatake, commercial research support, honoraria, Chugai Pharmaceutical Co., Ltd.

Acknowledgments

We thank Sayuri Minowa and Harumi Shibata for their assistance in specimen preparation from lymph node biopsies; Chie Watanabe for help with the statistics; and Dr. Dovie Wylie of On-site English, Inc. (Palo Alto, CA) for English editing assistance.

References

1. Golay J, Zaffaroni L, Vaccari T, et al. Biologic response of B lymphoma cells to anti-CD20 monoclonal antibody rituximab *in vitro*: CD55 and CD59 regulate complement-mediated cell lysis. Blood 2000;95:3900–8.
2. Fischer L, Penack O, Gentilini C, et al. The anti-lymphoma effect of antibody-mediated immunotherapy is based on an increased degranulation of peripheral blood natural killer (NK) cells. Exp Hematol 2006;34:753–9.
3. Coiffier B. Monoclonal antibodies combined to chemotherapy for the treatment of patients with lymphoma. Blood Rev 2003;17:25–31.
4. Cragg MS, Glennie MJ. Antibody specificity controls *in vivo* effector mechanisms of anti-CD20 reagents. Blood 2004;103:2738–43.
5. Zhang N, Khawli LA, Hu P, Epstein AL. Generation of rituximab polymer may cause hyper-cross-linking-induced apoptosis in non-Hodgkin's lymphomas. Clin Cancer Res 2005; 11:5971–80.
6. Pedersen IM, Buhl AM, Klausen P, Geisler CH, Jurlander J. The chimeric anti-CD20 antibody rituximab induces apoptosis in B-cell chronic lymphocytic leukemia cells through a p38 mitogen activated protein-kinase-dependent mechanism. Blood 2002;99:1314–9.
7. Hatjiharissi E, Xu L, Santos DD, et al. Increased natural killer cell expression of CD16, augmented binding and ADCC activity to rituximab among individuals expressing the Fc{γ}RIIIa-158 V/V and V/F polymorphism. Blood 2007;110:2561–4.
8. Treon SP, Hansen M, Branagan AR, et al. Polymorphisms in FcγRIIIA (CD16) receptor expression are associated with clinical response to rituximab in Waldenstrom's macroglobulinemia. J Clin Oncol 2005;23:474–81.
9. Dall'Ozzo S, Tartas S, Paintaud G, et al. Rituximab-dependent cytotoxicity by natural killer cells: influence of FCGR3A polymorphism on the concentration-effect relationship. Cancer Res 2004;64:4664–9.
10. Cartron G, Dacheux L, Salles G, et al. Therapeutic activity of humanized anti-CD20 monoclonal antibody and polymorphism in IgG Fc receptor FcγRIIIa gene. Blood 2002;99:754–8.
11. Bannerji R, Kitada S, Flinn IW, et al. Apoptotic-regulatory and complement-protecting protein expression in chronic lymphocytic leukemia: relationship to *in vivo* rituximab resistance. J Clin Oncol 2003;21:1466–71.
12. Terui Y, Sakurai T, Mishima Y, et al. Blockade of bulky lymphoma-associated CD55 expression by RNA interference overcomes resistance to complement-dependent cytotoxicity with rituximab. Cancer Sci 2006;97:72–9.
13. Harjunpaa A, Junnikkala S, Meri S. Rituximab (anti-CD20) therapy of B-cell lymphomas: direct complement killing is superior to cellular effector mechanisms. Scand J Immunol 2000;51:634–41.
14. van Meerten T, van Rijn RS, Hol S, Hagenbeek A, Ebeling SB. Complement-induced cell death by rituximab depends on CD20 expression level and acts complementary to antibody-dependent cellular cytotoxicity. Clin Cancer Res 2006;12: 4027–35.
15. Byrd JC, Kitada S, Flinn IW, et al. The mechanism of tumor cell clearance by rituximab *in vivo* in patients with B-cell chronic lymphocytic leukemia: evidence of caspase activation and apoptosis induction. Blood 2002;99:1038–43.

16. Stel AJ, Ten Cate B, Jacobs S, et al. Fas receptor clustering and involvement of the death receptor pathway in rituximab-mediated apoptosis with concomitant sensitization of lymphoma B cells to fas-induced apoptosis. J Immunol 2007;178: 2287–95.
17. Weng WK, Levy R. Two immunoglobulin G fragment C receptor polymorphisms independently predict response to rituximab in patients with follicular lymphoma. J Clin Oncol 2003;21: 3940–7.
18. Anolik JH, Campbell D, Felgar RE, et al. The relationship of FcγRIIIa genotype to degree of B cell depletion by rituximab in the treatment of systemic lupus erythematosus. Arthritis Rheum 2003;48:455–9.
19. Clynes RA, Towers TL, Presta LG, Ravetch JV. Inhibitory Fc receptors modulate *in vivo* cytoxicity against tumor targets. Nat Med 2000;6:443–6.
20. Anderson DR, Grillo-Lopez A, Varns C, Chambers KS, Hanna N. Targeted anti-cancer therapy using rituximab, a chimaeric anti-CD20 antibody (IDEC-C2B8) in the treatment of non-Hodgkin's B-cell lymphoma. Biochem Soc Trans 1997;25:705–8.
21. Di Gaetano N, Cittera E, Nota R, et al. Complement activation determines the therapeutic activity of rituximab *in vivo*. J Immunol 2003;171: 1581–7.
22. van der Kolk LE, Grillo-Lopez AJ, Baars JW, Hack CE, van Oers MH. Complement activation plays a key role in the side-effects of rituximab treatment. Br J Haematol 2001;115:807–11.
23. Weng WK, Levy R. Expression of complement inhibitors CD46, CD55, and CD59 on tumor cells does not predict clinical outcome after rituximab treatment in follicular non-Hodgkin lymphoma. Blood 2001;98:1352–7.